Excited-state relaxation in π-conjugated polymers

S. V. Frolov and Z. Bao
Bell Laboratories, Lucent Technologies, 600 Mountain Avenue, Murray Hill, New Jersey 07974

M. Wohlgenannt and Z. V. Vardeny
Physics Department, University of Utah, Salt Lake City, Utah 84112

(Received 1 September 2000; revised manuscript received 3 November 2000; published 20 May 2002)

We study ultrafast relaxation processes of odd- (B_u) and even-parity (A_g) exciton states in poly(*p*-phenylene vinylene) derivatives. The B_u states are studied using a regular two-beam pump-and-probe spectroscopy, which can monitor vibronic relaxation and exciton diffusion. In order to observe the A_g states, a three-beam femtosecond transient spectroscopy is developed, in which two different excitation pulses successively generate odd-parity ($1B_u$) excitons at 2.2 eV and then reexcite them to higher A_g states. We are able to distinguish two different classes of A_g states: one class (mA_g) experiences ultrafast internal conversion back to the lowest singlet exciton, whereas the other class (kA_g) in violation of the Vavilov-Kasha's rule undergoes a different relaxation pathway. The excitons subsequently dissociate into long-lived polaron pairs, which results in emission quenching with the action spectrum similar to that of the intrinsic photoconductivity. We conclude that the A_g states above 3.3 eV (kA_g) are charge-transfer states, that mediate carrier photogeneration.

DOI: 10.1103/PhysRevB.65.205209 PACS number(s): 78.47.+p, 78.55.Kz, 78.30.Jw

I. INTRODUCTION

Optical properties of luminescent π-conjugated polymers have been extensively studied in the past 20 years. By and large, they have been found to be similar to those of large centrosymmetric molecules. Polymer photophysics is therefore determined by a series of alternating odd- (B_u) and even- (A_g) parity excited states,[1] corresponding to one-photon and two-photon allowed transitions, respectively. Optical excitation into either of these states is followed by subpicosecond nonradiative relaxation to the lowest excited state.[2] This relaxation is due to either vibrational cooling within vibronic sidebands of the same electronic state or phonon-assisted transitions between two different electronic states. In molecular spectroscopy, the latter process is termed internal conversion. Internal conversion is usually the fastest relaxation channel, providing efficient nonradiative transfer from a higher excited state to the lowest excited state of the same spin multiplicity. As a result, the vast majority of molecular systems follow the Vavilov-Kasha rule, stating that fluorescence typically occurs from the lowest excited electronic state and its quantum yield is independent of the excitation wavelength.[3]

Luminescent π-conjugated polymers, like many other complex molecular systems, are expected to follow the Vavilov-Kasha rule. The independence of exciton generation yield on the excitation wavelength has indeed been demonstrated for poly(*p*-phenylene vinylene) (PPV) type polymers.[4] This observation has indicated that internal conversion is likely to be the dominant relaxation channel between different excited states in π-conjugated polymers. A similar situation occurs in organic molecular crystals, where intramolecular internal conversion is by far the fastest relaxation process.[5] However, there are other processes that may interfere and successfully compete with internal conversion. Among the known competing processes are singlet exciton fission and exciton dissociation.[6] The first process creates two triplet excitons with opposite spins, whereas the latter produces charge carriers.

In this work we use a multiple-excitation transient spectroscopy to study the relaxation between different excited states in a typical luminescent π-conjugated polymer, derivatized PPV. Although our study primarily concentrates on thin polymer films, some of the measurements are also done on polymer chains in solution. We investigate the relaxation within the excitation manifolds of B_u and A_g states. We identify prominent bands of two different A_g states, mA_g at ~3.2 eV and kA_g at ~3.6 eV, using both two-photon absorption and transient photomodulation spectroscopies. We find that whereas mA_g obeys the Vavilov-Kasha rule and decays back to $1B_u$ via internal conversion within 200 fs, kA_g exhibits anomalous behavior and relaxes into a longer-lived, nonemissive state, which is attributed to a bound electron-hole polaron pair. This nontrivial result indicates that kA_g may be categorized as a charge-transfer state; such states are thought to be a prerequisite for carrier photogeneration. This conclusion is supported by transient photomodulation spectra and a comparison between the action spectra of photoluminescence quenching and photoconductivity. Section II describes the experimental techniques used in this work. In Sec. III, we use both steady-state and transient absorption to characterize the excited states of PPV polymers. In Secs. IV and V we study the relaxation dynamics of odd- and even-parity states, respectively. Section V particularly concentrates on the three-beam transient spectroscopy. The results are summarized in Sec. VI.

II. EXPERIMENTAL SETUP

In our studies we focus on two different PPV derivatives: dioctyloxy-PPV (DOO-PPV) (Ref. 7) and dendritic side-chain substituted PPV (PPVD0) (Ref. 8). Polymer films (thickness of 0.5–1 μm) are prepared by evaporation from polymer solutions in chloroform (~1 mg/ml) via either drop-

casting or spin-coating onto quartz substrates. These polymer films are prone to photo-oxidation. In order to reduce photo-oxidation, all measurements are done in flowing N_2, at room temperature.

A pump-and-probe correlation technique is used to obtain time-resolved photomodulation (PM) spectra by measuring $\Delta T(t)/T$ versus the probe photon energy $\hbar\omega$, where T is the probe transmission, ΔT is the change in T due to the pump pulse, and t is the time delay between the pump and probe pulses. Negative ΔT implies photoinduced absorption (PA), whereas positive ΔT is due to either photobleaching or probe-induced stimulated emission (SE). Two electronically synchronized Ti:sapphire mode-locked lasers (Spectra-Physics Tsunami), one of which pumps an optical parametric oscillator (Opal), are used to produce 100-fs pump and probe pulses at a repetition rate of 80 MHz. Electronic synchronization is limited to 6 ps by the pulse jitter. In measurements requiring subpicosecond resolution the pump and probe beams are produced by a single Ti:sapphire laser (and the Opal oscillator if necessary). The excitation $\hbar\omega$ can vary between 2.5 and 3.2 eV; the probe $\hbar\omega$ can be continuously changed from 0.55 to 2.2 eV and from 0.11 to 0.21 eV. In the measurements of transient PM spectra, the pump and probe beam polarizations are parallel to each other. Typical photoexcitation densities are below $10^{17}\,\mathrm{cm}^{-3}$, so that $\Delta T/T$ does not exceed 3×10^{-4}.

III. GROUND- AND EXCITED-STATE ABSORPTION IN PPV

Figure 1(a) shows the one- and two-photon absorption spectra, $\alpha(\hbar\omega)$, of DOO-PPV and PPVD0 films. Absorption bands marked I, II, III, and IV in the one-photon absorption spectra are observed in virtually all PPV derivatives.[9] These bands have been identified as optical transitions between π(occupied) and π^*(unoccupied) molecular orbitals (MO's).[10] MO's in PPV polymers have been traditionally classified as delocalized (d and d^*) and localized (l and l^*); the former are delocalized across all carbon atoms, whereas the latter have nodes at para positions of the benzene rings, which results in charge confinement at the rings.[11] Calculations show that bands I and II originate from $d\rightarrow d^*$ transitions,[9] band IV is due to $l\rightarrow l^*$, and band III involves degenerate transitions $d\rightarrow l^*$ and $l\rightarrow d^*$.[11] A PPV chain is a molecular system with a center of inversion; thus its excited states have been classified as A_g (gerade) and B_u (ungerade). Since the polymer ground state is described by a totally symmetric wave function (i.e., an A_g state), optical transitions are allowed only to the B_u states (states of the opposite parity). Thus band I in Fig. 1 describes the lowest allowed state, i.e., $1B_u$ exciton at $E(1B_u)=2.2\,\mathrm{eV}$.[12] Excitation to bands II–IV produces higher B_u states with very different electron-hole distributions.[13,14] Each of these excited states have different potential energy surfaces (the energy dependence on the nuclear coordinates), and therefore their relaxation pathways may differ.

The A_g states, which are not observable by one-photon absorption, can be found from the two-photon absorption spectrum shown in the Fig. 1(a) inset for the DOO-PPV

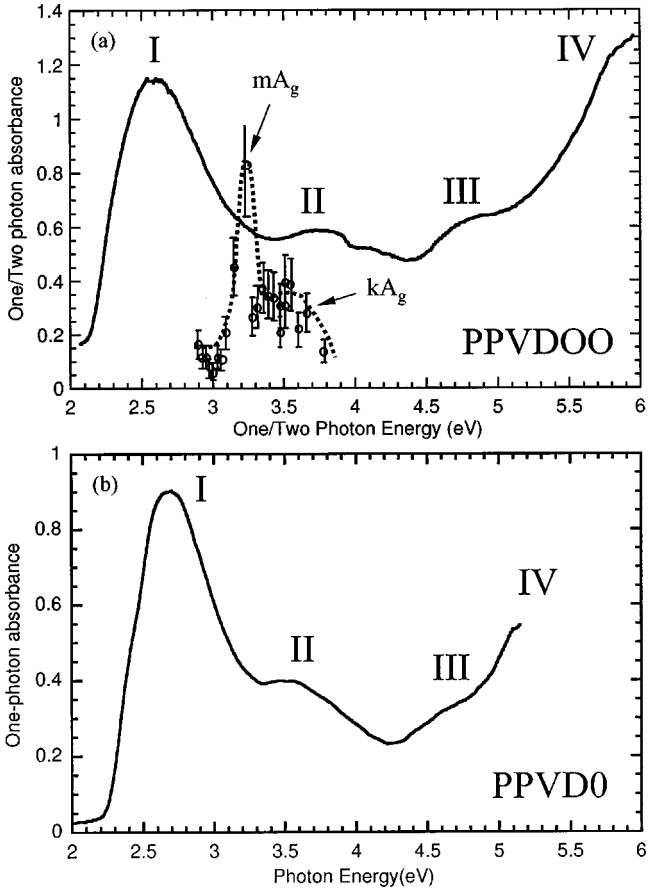

FIG. 1. (a) One-photon (solid line) absorbance of a DOO-PPV film and two-photon (circles) absorption of DOO-PPV in solution; (b) one-photon absorbance spectrum of a PPVD0 film. Bands I, II, III, and IV, as well as mA_g and kA_g states are assigned.

solution.[15] This spectrum was obtained in DOO-PPV solutions using a Z-scan technique.[15] From these measurements, as well as electroabsorption measurements,[12] we find two prominent two-photon allowed states, mA_g and kA_g, at $E(mA_g)\approx3.1\,\mathrm{eV}$ and $E(kA_g)\approx3.5\,\mathrm{eV}$, respectively. The theory of A_g states in PPV polymers is less developed as compared to that of B_u states, partly due to the scarcity of the relevant experimental data. Several recent theoretical studies, however, have attempted to elucidate the complex nature of the A_g states in PPV.[16,17] These calculations show a broad manifold of A_g states, only two of which appear prominently in the nonlinear optical spectroscopy (two-photon or electroabsorption). Since these states are two-photon allowed, they should also appear in the PA spectrum of $1B_u$ excitons.

Figure 2 shows the transient PM spectra of DOO-PPV and PPVD0 films measured at $t=2$ ps, where the prominent features can be assigned to optical transitions of the relaxed $1B_u$ excitons. These features include a vibronically broadened SE band at $\hbar\omega>1.7\,\mathrm{eV}$ and two PA bands at $\hbar\omega<1.7\,\mathrm{eV}$ marked PA_1 and PA_2, as shown in Fig. 2. The SE band closely resembles the photoluminescence (PL) spectrum and thus describes the radiative transitions of the $1B_u$ exciton to the ground state ($1A_g\leftarrow1B_u$).[7] Bands PA_1 and PA_2 have been attributed to transitions from $1B_u$ to mA_g and

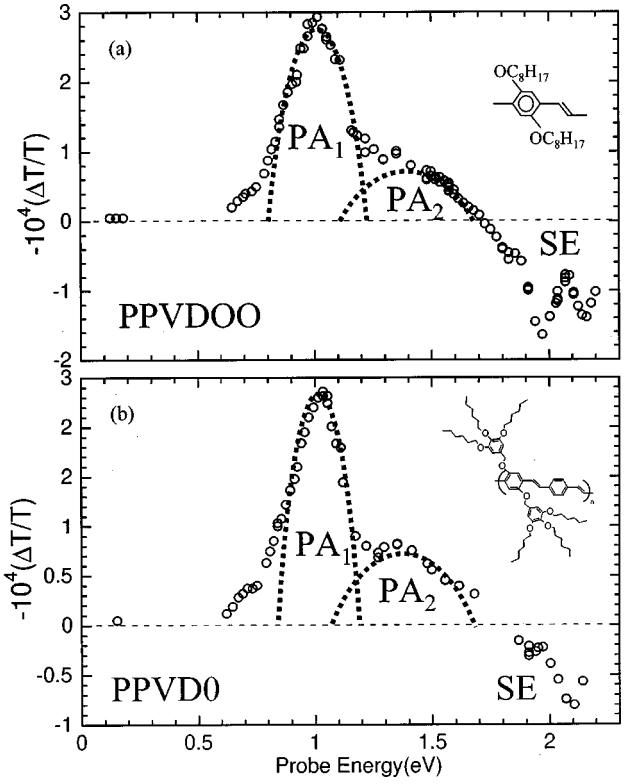

FIG. 2. Transient PM spectra of (a) DOO-PPV and (b) PPVD0 films at $t=2$ ps. DOO-PPV and PPVD0 repeat units are shown in the upper and lower insets, respectively. The dashed lines schematically mark the PA_1 and PA_2 bands.

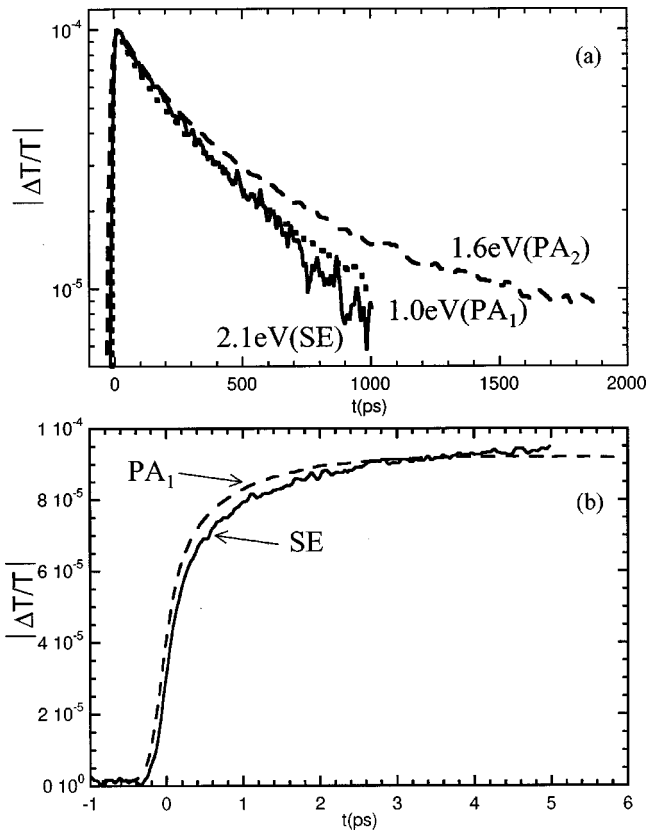

FIG. 3. (a) $\Delta T/T$ decays at $\hbar\omega=2.1$ eV (solid line), 1.6 eV (broken line), and 1.0 eV (dashed line) in PPVD0 films; (b) SE (solid line) and PA_1 (broken line) rise dynamics in PPVD0 films.

kA_g, respectively.[7,18] Indeed, the peak positions of PA_1 at 1.0 eV and PA_2 at 1.4 eV match with the energy differences between the two A_g states and $1B_u$ [see Fig. 1(a)]. Furthermore, the decay dynamics of the SE, PA_1, and PA_2 bands are identical up to ~300 ps, as shown in Fig. 3(a) for the PPVD0 film. Similar results are obtained for the DOO-PPV films.[7]

In general, the PA_2 dynamics differ from those of either SE or PA_1, due to contributions from other species such as triplets, polarons, and polaron pairs.[19,20] Specifically, in the case of pristine PPVD0 films, band PA_2 appears to have a long-lived component, which is also observed in DOO-PPV.[7] The long-lived component has been attributed to triplet excitons produced from the singlet excitons via intersystem crossing.[7] There are also discrepancies between the PA_1 and PA_2 dynamics on the subpicosecond time scale, which are discussed further below. The match between the PA_1 and SE dynamics, on the other hand, is almost perfect. Their picosecond decays are virtually identical, and the rise-time dynamics are also very close to each other, as shown in Fig. 3(b). From the picosecond decay we infer the average exciton lifetime τ to be about 200 ps for DOO-PPV and 300 ps for the PPVD0 films, respectively.

A midinfrared (ir) spectral range between 0.11 and 0.21 eV deserves special attention. This region corresponds to the absorbtion of ir-active vibrations (IRAV), which are regularly used for the identification of charge excitations.[21] We find a small transient PM signal in this range with a flat, featureless spectrum (only three points are shown for DOO-PPV and one point for PPVD0 in Fig. 2). This transient mid-IR PM response cannot be attributed to the IRAV modes, which are characterized by several pronounced narrow lines.[21] In Fig. 4 we compare the PA dynamics at 8.2 μm (0.15 eV) with the PA dynamics at 1.0 eV: both PA decays [Fig. 4(a)] and onsets [Fig. 4(b)] are identical. We therefore attribute the mid-ir PM response to $1B_u$ absorption, possibly the low-energy tail of the excitonic PA_1 band.

IV. EXCITED-STATE RELAXATION DYNAMICS

We adopt the nomenclature of molecular spectroscopy to describe the excitation and relaxation processes in PPV derivatives, since the polymer photophysics is similar to the photophysics of large organic molecules. Figure 5 shows schematically the configuration coordinate diagram of all identifiable low-energy states in the family of PPV derivatives. Due to the coupling to the nuclear coordinates (described by an effective configuration coordinate), each electronic state is characterized by a potential energy surface as shown by the parabolas in Fig. 5. In this diagram the most probable optical transition corresponds to the vertical line connecting two different energy surfaces of opposite parities. We distinguish several excitation manifolds, marked by dashed boxes: the inhomogeneously broadened lowest singlet exciton ($1B_u$), the manifold of A_g states (mA_g through kA_g), the lowest triplet exciton ($1\ ^3B_u$), and the manifold of

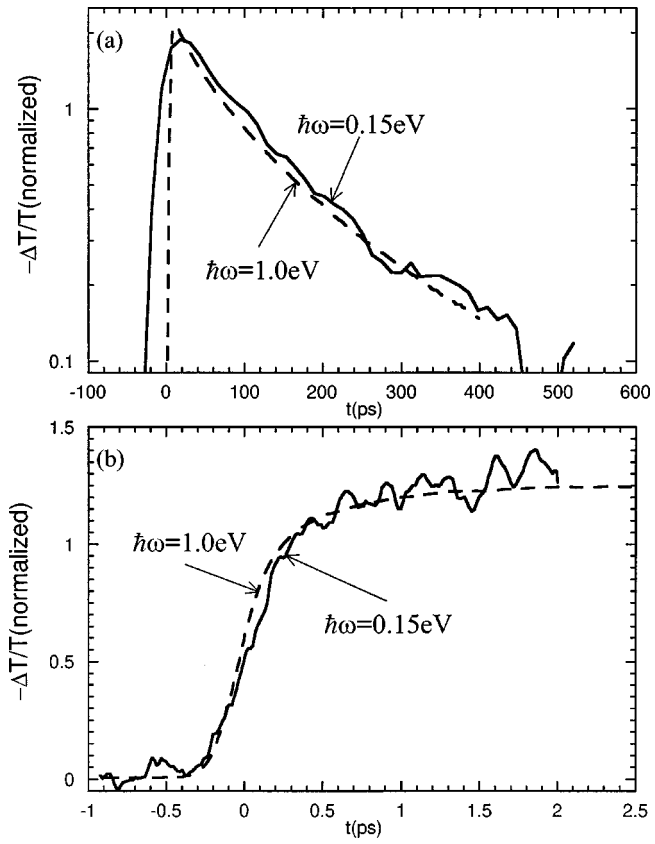

FIG. 4. (a) $\Delta T/T$ decays at $\hbar\omega = 0.15$ eV (solid line) and 1.0 eV (broken line) in DOO-PPV films; (b) $\Delta T/T$ rise dynamics at $\hbar\omega = 0.15$ eV (solid line) and 1.0 eV (broken line) in DOO-PPV films.

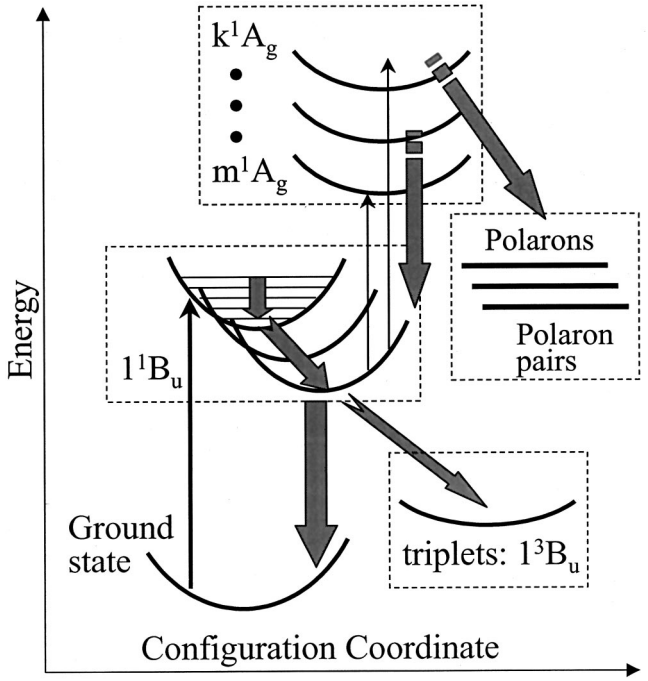

FIG. 5. Configuration coordinate diagram of low-energy excited states in PPV polymers: various excitation manifolds are marked by dashed line boxes. Narrow vertical arrows show optical transitions, whereas broad arrows indicate nonradiative relaxation pathways.

charge excitations and charge-transfer states (polarons and polaron pairs). Other B_u states are not shown, since they are not closely investigated in this work. In this description we assume that the essential photophysics is given by intrachain interactions and ignore possible complications due to interchain interactions. This assumption is supported by the similarity between optical properties of solid films and dilute solutions.[7,20]

π-conjugated polymers are generally characterized by significant inhomogeneous broadening.[22] This is particularly evident from the featureless band I in the linear absorption spectra (Fig. 1), which should appear as a well-defined vibronic progression based on the $1B_u$ exciton. Instead, the distribution in the chain conjugation length leads to a broad distribution of $1B_u$ energies, which in turn smoothens out the vibronic structure of band I. This disorder also hinders the accurate identification of other excited states above $1B_u$. The disorder is due to both polymer chain length fluctuations and conjugation length distribution within a single chain (determined by the amount of kinks and other defects on the chain). Inhomogeneous broadening thus opens an additional relaxation pathway for the excited states, which consequently results in both spectral and spatial diffusion of excitation in the polymer.[22] The diffusion occurs in the direction of longer conjugation chain segments, where the energy is the lowest.

In our pump-and-probe measurements, the highest pump photon energy is 3.2 eV, which is not high enough to reach band II (see Fig. 1). Thus in single-pump experiments, we only achieve excitations into band I, i.e., the $1B_u$ excitation manifold. Following this photoexcitation, excitons experience vibrational cooling and move to the bottom of their potential energy surfaces by emitting phonons and changing the equilibrium configuration coordinates (Fig. 5). Simultaneously, there may be energy transfer between segments of different conjugation lengths, resulting in exciton spectral diffusion towards the lowest possible energy surface. The energy transfer can be coherent, if there is an overlap between exciton wave functions of the two chain segments, e.g., when these segments belong to the same polymer chain. Alternatively, in the case of two well-separated polymer chains, the energy transfer between them could be due to the incoherent Förster transfer.[23]

Relaxation within the $1B_u$ manifold can be studied by monitoring the femtosecond dynamics of SE, PA_1, or PA_2, which approximately follow the $1B_u$ population dynamics. Additional information about relaxation can be obtained from the polarization anisotropy decay, which we define as a ratio between PM components with the probe beam polarizations parallel (XX) and perpendicular (XY) to the pump beam polarization. Figure 6 shows the PA_1 dynamics in DOO-PPV films on picosecond and subpicosecond time scales for two probe polarizations and the ratios between them. As shown in Fig. 3(b), the onset of excitonic PA_1 mimics the behavior of excitonic SE. Its rise time is easily resolved with our 100-fs pump and probe pulses. The excitation energy in these measurements is 3.2 eV, which means that photoexcitation occurs into the highest vibronic sidebands of the $1B_u$

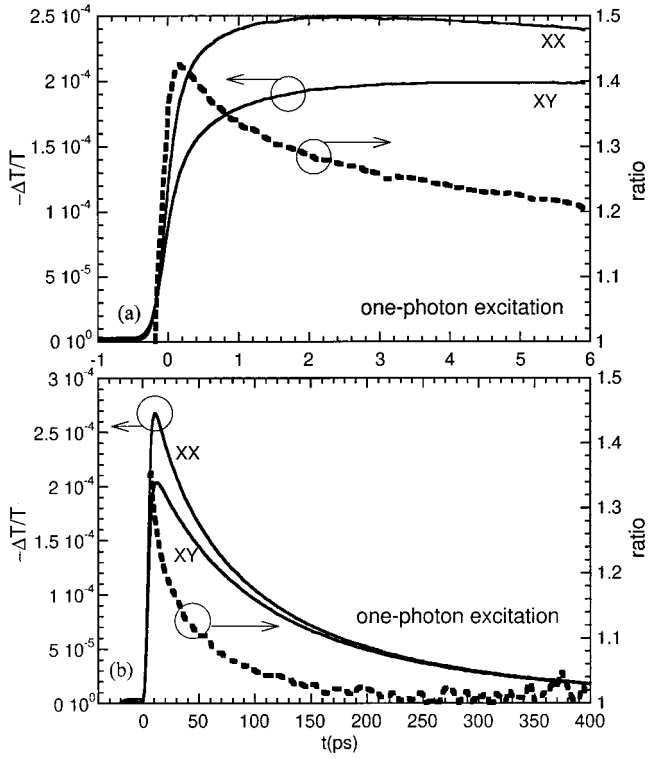

FIG. 6. Polarized PA_1 dynamics at 1.0 eV following one-photon excitation (left scale) for the probe polarization parallel (*XX*) and perpendicular (*XY*) to the pump polarization, and the polarization anisotropy ratio (right scale) in DOO-PPV films, on (a) short and (b) long time scales.

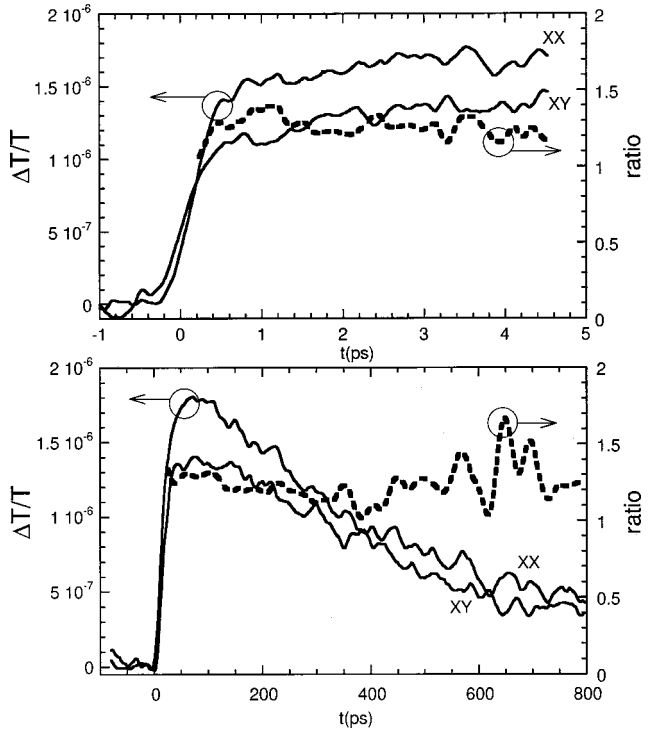

FIG. 7. Polarized PA_1 dynamics at 1.0 eV following one-photon excitation (left scale) for the probe polarization parallel (*XX*) and perpendicular (*XY*) to the pump polarization, and the polarization anisotropy ratio (right scale) in DOO-PPV dilute solutions on (a) short and (b) long time scales.

exciton and possibly some other allowed states (nB_u) below band II. Since the shorter chain segments have higher $1B_u$ energies, this excitation may also preferentially excite short conjugation chain segments. Thus subsequent relaxation of inhomogeneously broadened, vibrationally hot $1B_u$ excitons should include phonon emission and exciton diffusion among different chain segments. The former affects the PA_1 magnitude, whereas the latter reveals itself in the decay of polarization anisotropy.

Accordingly, the PA_1 onset (and also the SE onset) dynamics can be attributed to cooling towards the new configuration equilibrium within the $1B_u$ manifold. This vibrational relaxation initially occurs with a time constant of 300 fs, which is followed by a slower component with a time constant of 830 fs. The onset dynamics may also be influenced by the exciton diffusion. However, the polarization decay on the subpicosecond time scale shows a slower dynamics characterized by a time constant of 1.65 ps, suggesting that the exciton spatial diffusion occurs on a longer time scale as compared to that of the intrachain exciton cooling. As shown in Fig. 6(b), the polarization ratio decay, and thus spatial diffusion, continue until band PA_1 becomes isotropic at about 150 ps. In an attempt to separate the intrachain (vibrational) and interchain (diffusion) relaxation channels within the $1B_u$ excitation manifold, we measure the PA_1 decay and polarization anisotropy in a very dilute solution of DOO-PPV in chloroform (a few milligrams per liter). Figure 7 shows the polarized PA_1 dynamics in the DOO-PPV solution on picosecond and subpicosecond time scales (the poor sensitivity is due to the low DOO-PPV concentration in the solution). A major difference between the dynamics in films and solutions is found in the decay of polarization anisotropy. The PA_1 anisotropy in solution is completely preserved, at least up to 1 ns. This indicates that PPV chains in solution are uncoiled and straight, and that exciton diffusion is limited to the diffusion within single chains, suspended and isolated from each other by the solvent. On the other hand, the PA_1 onset in solutions is very similar to that in films, which indicates that the PA_1 subpicosecond dynamics in films are primarily determined by the intrachain processes. Therefore, we conclude that spectral relaxation resulting from the interchain diffusion is negligible in our films within at least the first few picoseconds.

Similarly, we can use the PA_2 dynamics to study the $1B_u$ relaxation. However, the PA_2 subpicosecond dynamics are very different from those of PA_1 and SE. Figure 8(a) shows the polarized PA_2 dynamics and the decay of the polarization anisotropy in DOO-PPV films. The polarization anisotropy decay at 1.6 eV (PA_2) is about the same as that at 1.0 eV (PA_1) (compare with Fig. 6) and thus describes the same dynamics due to spatial diffusion. However, unlike PA_1 or SE, PA_2 rises instantaneously after the excitation pulse and then experiences partial ultrafast decay. This ultrafast PA_2 decay has a time constant of 800 fs and matches the slower component of the PA_1 onset. Similar dynamics, shown in Fig. 8(c), are observed in DOO-PPV solutions; the ultrafast PA_2 decay and PA_1 rise are slower in solution by factor of 5.

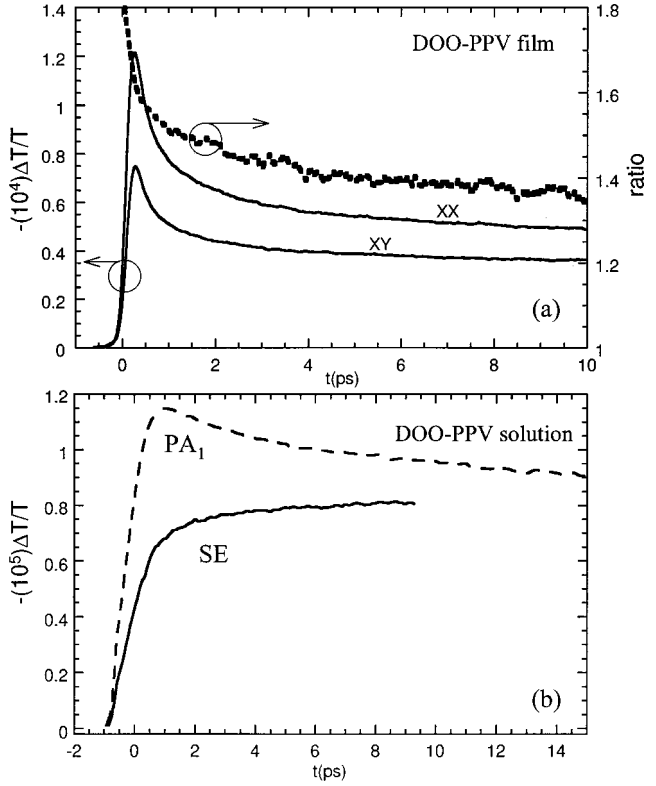

FIG. 8. (a) Polarized PA_2 dynamics at 1.6 eV following one-photon excitation (left scale) for the probe polarization parallel (*XX*) and perpendicular (*XY*) to the pump polarization, and the polarization anisotropy ratio (right scale) in DOO-PPV films. (b) SE (solid line) and PA_1 (broken line) dynamics in DOO-PPV solutions.

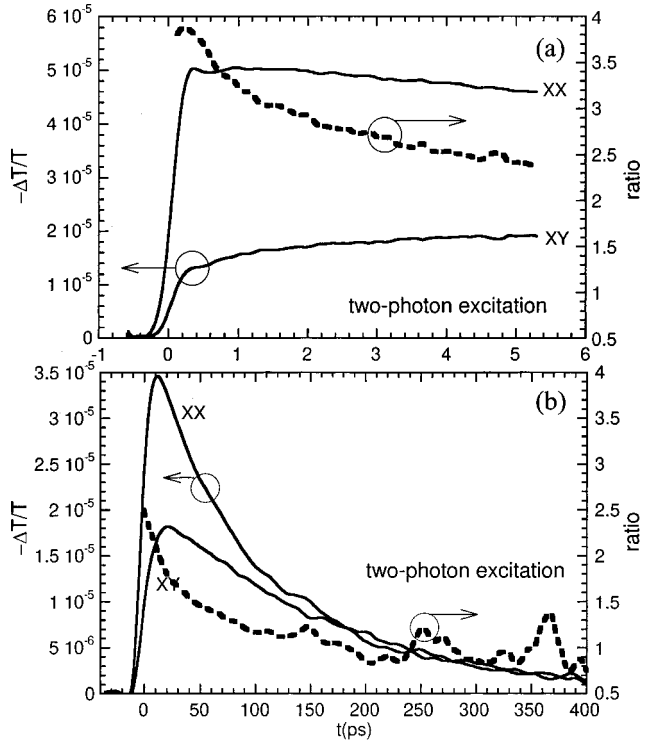

FIG. 9. Polarized PA_1 dynamics at 1.0 eV following two-photon excitation (left scale) for the probe polarization parallel (*XX*) and perpendicular (*XY*) to the pump polarization, and the polarization anisotropy ratio (right scale) in DOO-PPV films on (a) short and (b) long time scales.

We suggest that the PA_2 ultrafast decay is due to the spectral relaxation within the distribution of different conjugated segments on the same polymer chain. In the regions with shorter conjugation length, the $1B_u$ energy increases due to the confinement effect.[24] One may expect a similar effect on the transition energy $E(1B_u \rightarrow mA_g)$, which would blueshift the PA_1 band in shorter chain segments and spectrally overlap it with PA_2 in longer chain segments. Since PA_1 is much stronger than PA_2, this would result in a relatively higher PA signal observed at 1.4–1.6 eV immediately after pulsed photoexcitation. Subsequent ultrafast energy transfer to the longer chain segments is then observed as the fast partial decay of PA_2 and the simultaneous rise of PA_1. The difference between the characteristic time constants of 0.8 ps in films and ~5 ps in solution can be attributed to inefficient heat exchange between PPV chains and the solvent. In films neighboring chains provide an efficient heat sink and quickly cool the excitons, whereas in solution the cooling rate is slower and thus ''hot'' excitons may revisit the energetically higher, shorter chain segments.

In order to study the relaxation within excitation manifolds other than $1B_u$, we have to apply a different excitation method. For example, two-photon absorption is required to reach any state that belongs to the A_g manifold. In our pump-and-probe measurements, we can use the pump pulses with photon energy below the optical gap, so that the excitation occurs only via a two-photon allowed transition. With the pump energy of 1.6 eV, we thus can directly access the mA_g state at 3.2 eV (see Fig. 5). Figure 9 shows the observed polarized PA_1 dynamics following the two-photon excitation into mA_g in DOO-PPV films. We observe much higher polarization anisotropy, as expected for the two-photon nonlinear process; its decay, however, is similar to that obtained with the one-photon excitation (Fig. 6). The main difference between the two-photon and one-photon excited PA_1 dynamics is the apparent instantaneous onset of PA_1 in the case of two-photon excitation. We believe this fast PA_1 rise is due to PA, which originates directly from the mA_g state and spectrally overlaps with the PA_1 band of the $1B_u$ excitons. The decay of this PA component (due to the mA_g exciton decay) is faster than the subsequent rise of PA_1 (due to $1B_u$), which leads to the appearance of a small dip at $t \sim 0.5$ ps [see Fig. 9(a)]. Similar results are also obtained using PPVD0 films, which are shown in Fig. 10. We can conclude from these measurements that the relaxation from mA_g to $1B_u$ is ultrafast and comparable to the rate of vibrational cooling of $1B_u$ excitons (300 fs). The mA_g state has its own PA spectrum, which, however, overlaps with the broad PA spectrum of $1B_u$ excitons. Both of these factors prevent an accurate determination of intrinsic relaxation dynamics within the A_g manifold. A multiple-excitation technique, which is discussed in the next section, avoids this limitation.

V. MULTIPLE-PULSE TRANSIENT SPECTROSCOPY

In order to clarify the relaxation of the A_g states, we use a three-pulse transient PM technique to monitor the exciton

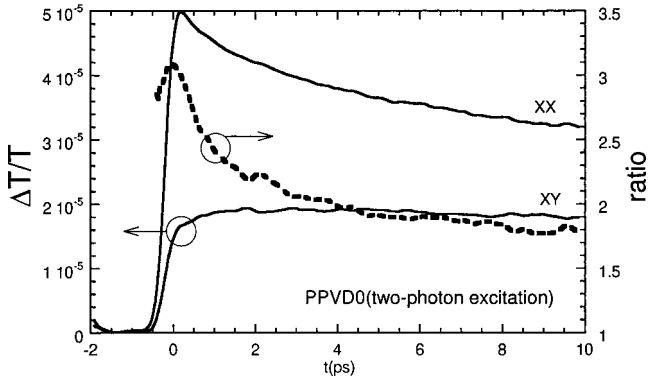

FIG. 10. Polarized PA_1 dynamics at 1.0 eV following two-photon excitation (left scale) for the probe polarization parallel (*XX*) and perpendicular (*XY*) to the pump polarization, and the polarization anisotropy ratio (right scale) in PPVD0 films.

dynamics following optical reexcitation from $1B_u$ to mA_g or kA_g.[18] In this technique, as shown in Fig. 11(a), $1B_u$ excitons are initially populated via excitation from the ground state by the first pump pulse (1) at $\hbar\omega_1 = E_1 > E(1B_u)$ and then reexcited after a delay time t_2 by a second pump pulse (2) at $\hbar\omega_2 = E_2$, tuned to a specific exciton transition (within PA_1 or PA_2 bands). The resulting exciton PM dynamics is monitored by a probe pulse (3) at $\hbar\omega_3 = E_3$ at a delay time t_3 using either an absolute or relative measuring mode. In the absolute mode ΔT due to both pump pulses is measured, whereas in the relative mode only the change, δT, due to the second pump pulse is detected using a double-frequency modulation (DM) technique.[25] For the DM technique, the first pump is modulated at 1 MHz and the second pump at 1 kHz, the signal (δT) is first electronically mixed with the 1-MHz square wave, and then measured with a lock-in amplifier referenced at 1 kHz. The second pump switching efficiency η can be defined as $|\delta T/\Delta T|$. Figure 11(b) shows the experimental setup, in which two Ti:sapphire mode-locked lasers and the synchronously pumped Opal oscillator produce the three pulses, e.g., the lower Ti:sapphire laser produces the frequency-doubled first pump pulse, the unused portion of the upper Ti:sapphire laser produces the second pump pulse, and the signal port of the Opal oscillator generates the probe pulse. In this arrangement, the jitter between the first and second pump pulses does not limit the temporal resolution of the recovery dynamics after reexcitation, since the second pump and probe pulses are perfectly synchronized. The two pump and one probe beam polarizations are parallel to each other. The laser beams are collinear and focused onto a small area of $\sim 20\ \mu$m in diameter. The average power of the second pump is kept low to avoid multiphoton excitation.

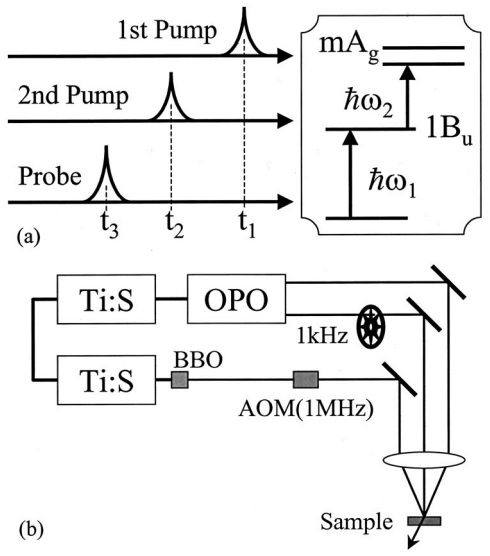

FIG. 11. (a) Schematic diagram of the three-beam photomodulation technique, showing two excitation pulses and one probe pulse, and the optical transitions induced by them in the polymer films. (b) Schematic diagram of the experimental setup used in the three-beam technique: Ti:S, Ti:sapphire lasers; OPO, optical parametric oscillator; BBO, barium borate doubling crystal; AOM, acousto-optic modulator.

We find that the relaxation dynamics of the A_g states in the DOO-PPV and PPVD0 films described below are virtually the same.[18] Therefore, in this work we only show results for either one of the two polymers, remembering that the data for the other polymer are essentially the same. As discussed previously, among the A_g states there are only two prominent states with strong dipole coupling to $1B_u$: mA_g and kA_g. We first study the relaxation of mA_g.

A. mA_g relaxation dynamics

The mA_g relaxation dynamics are measured following $1B_u$ reexcitation at $E_2 = 1.0$ eV (within PA_1) and four different t_2. The resulting decay of $1B_u$ population is observed by monitoring the SE dynamics (δSE) at $E_3 = 2.0$ eV, as shown in Fig. 12(a) for the PPVD0 film. We see that η is independent of t_2, which indicates that only $1B_u$ excitons are involved in the reexcitation process.[18] If any other excitation were responsible for the switching effect, for instance, with a shorter lifetime than the exciton lifetime, then η would be smaller for larger t_2. We find that mA_g quickly relaxes back to $1B_u$ by internal conversion with a time constant of about 200 fs [Fig. 12(a) inset]. The origin of a slower δT decay component with a time constant of ~ 3 ps is unclear. It may be attributed to $1B_u$ spatial transfer to the shorter chain segments due to the release of excess energy following internal conversion, and then subsequent diffusion back to the longer segments. However, we have shown previously that this process in films occurs in about 0.8 ps. Alternatively, the slower component could be due to the heating and subsequent cooling of the reexcited PPV chain. For $E_2 = 0.8-1.1$ eV over 99% of mA_g excitons recover back to $1B_u$ within 10 ps after reexcitation.

In addition to $1B_u$ depletion, as measured by transient δSE [Fig. 12(a) inset], we also observe concomitant transient PA from the reexcited mA_g excitons at $E_3 = 1.35-1.6$ eV with identical δPA dynamics to that of δSE. Figure 12(b) shows δPA_2 dynamics at $E_3 = 1.53$ eV following reexcitation into mA_g: an increase in PA (δPA) has the same decay as δSE and thus is attributed to the same process. This δPA can

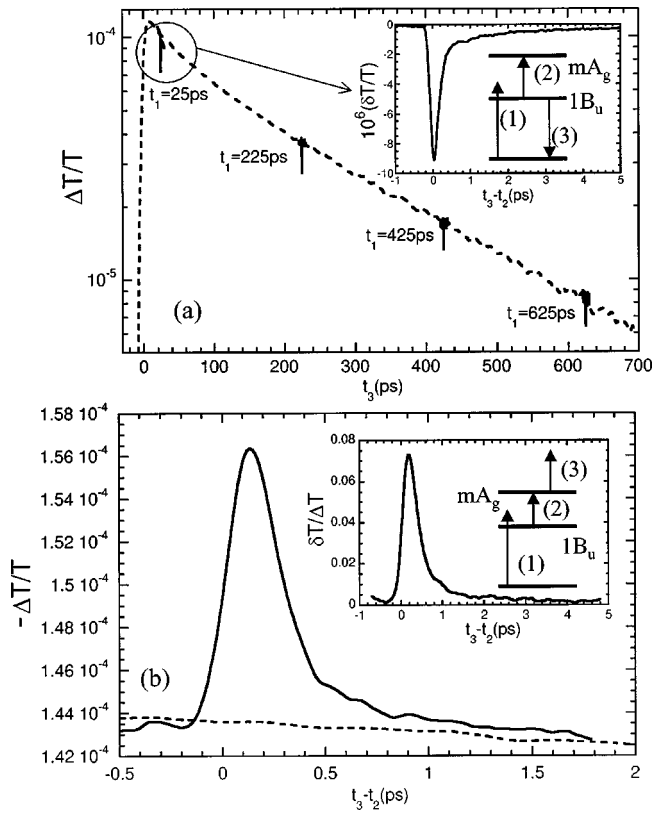

FIG. 12. (a) $\Delta T/T$ decay at $E_3=2.0$ eV without (broken line) and with (solid lines) the second pump pulse at $E_2=1.0$ eV, for four different t_2 in PPVD0 films; the inset shows the corresponding $\delta T/T$ decay and the experimental diagram. (b) $\Delta T/T$ decay at $E_3=1.6$ eV without (broken line) and with (solid lines) the second pump pulse at $E_2=1.0$ eV in PPVD0 films; the inset shows the corresponding $\delta T/T$ decay and the experimental diagram: 1, excitation by the first pump; 2, reexcitation by the second pump; and 3, absorption or emission induced by the probe pulses.

be tentatively assigned to a transition from mA_g into the B_u state corresponding to band III in Fig. 1, since $E(mA_g)+E_3=E(\text{bandIII})=4.7$ eV.

Very similar mA_g relaxation dynamics are measured in the dilute polymer solutions. Figure 13 shows the $1B_u$ recovery, as monitored by SE at 2.1 eV, in the PPVD0 solution in chloroform following reexcitation at $E_2=1.05$ eV. The ultrafast decay component of δSE is the same as that in films. However, the slower component in solutions is much more pronounced and longer lived than that in films (Fig. 13 inset). We believe that the origin of this discrepancy is the poor heat exchange in solutions. This observation supports the hypothesis that the slower component in the $1B_u$ recovery dynamics (from mA_g) represents the cooling of a reexcited PPV chain.

B. kA_g relaxation dynamics

We find drastically different δT dynamics when we increase E_2 up to 1.6 eV (within the PA_2 band) and access the kA_g state.[18] In these measurements we probe the $1B_u$ recovery dynamics at $E_3=0.6$–1.0 eV (within PA_1), as shown in

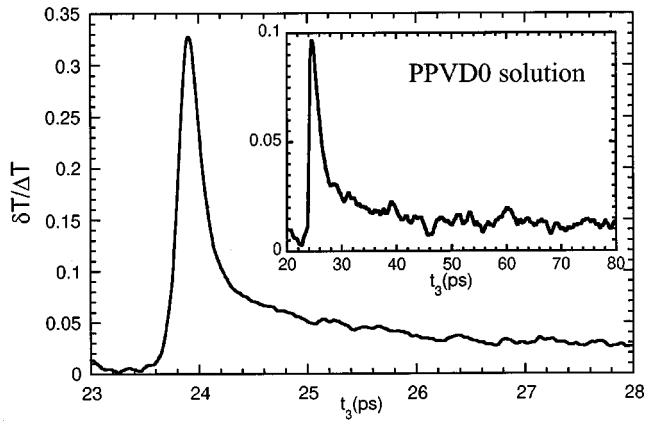

FIG. 13. $\delta T/\Delta T$ decay at $E_3=2.1$ eV with the second pump pulse at $E_2=1.05$ eV in PPVD0 solution; the inset shows the longer $\delta T/\Delta T$ decay.

Fig. 14(a) inset. Figure 14(a) shows the PA_1 dynamics with and without the second pump pulse at $E_2=1.6$ eV. Reexcitation into kA_g does not result in the ultrafast recovery of $1B_u$. Figure 14(b) shows the $1B_u$ population decay probed at $E_3=0.6$ eV (within PA_1) with and without the second

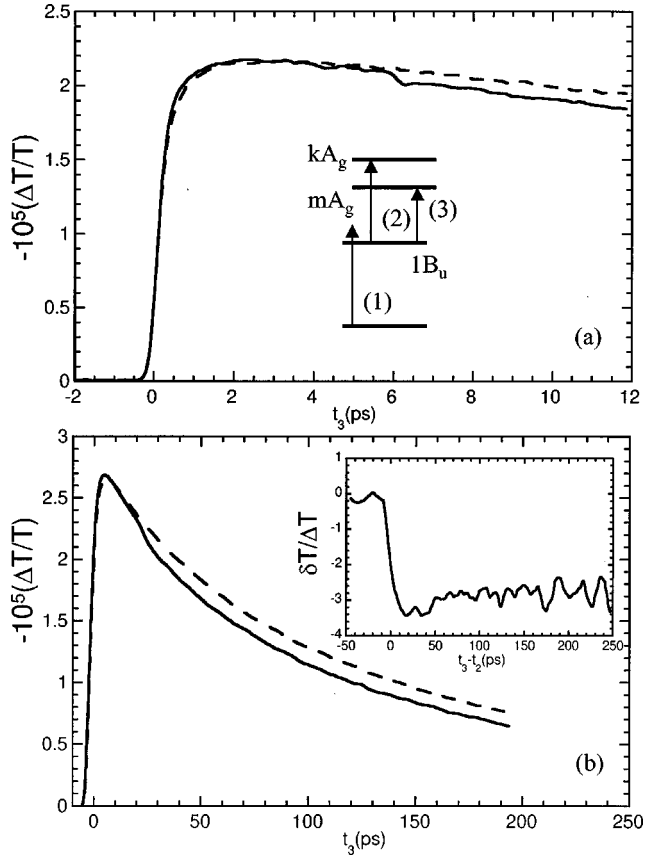

FIG. 14. (a) $\Delta T/T$ decay at $E_3=1.0$ eV without (broken line) and with (solid line) the second pump pulse at $E_2=1.6$ eV and $t_2=6$ ps in DOO-PPV films; the inset shows the experimental diagram. (b) $\Delta T/T$ decay at $E_3=0.6$ eV without (broken line) and with (solid line) the second pump pulse at $E_2=1.6$ eV and $t_2=25$ ps in DOO-PPV films; the inset shows the normalized δT decay.

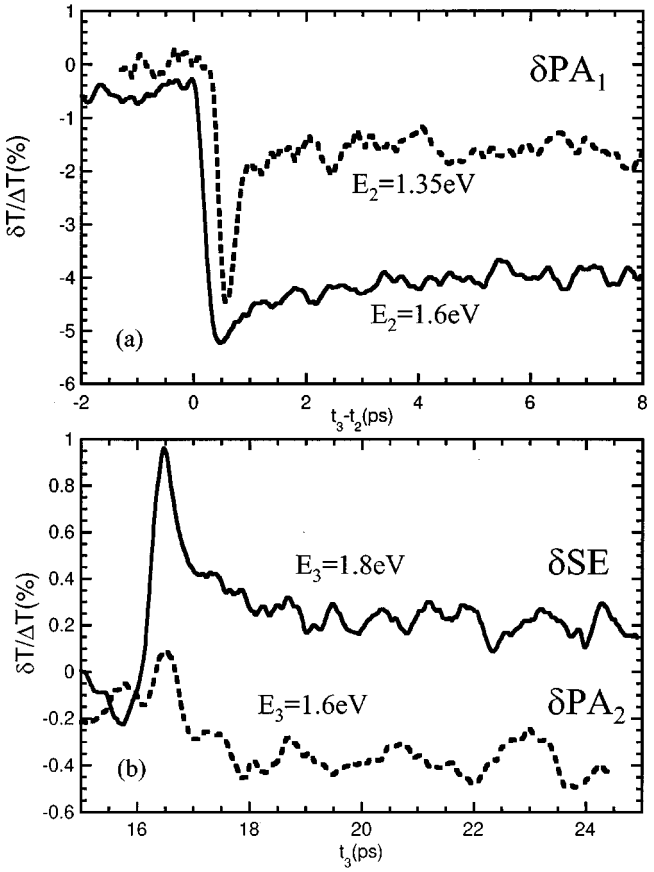

FIG. 15. (a) $\delta T/T$ decays for $E_2=1.6\,\mathrm{eV}$ (solid line) and $E_2=1.35\,\mathrm{eV}$ (dashed line) with $E_3=1.0\,\mathrm{eV}$ in DOO-PPV films. (b) δT decays with the second pump pulse at $E_2=1.5\,\mathrm{eV}$ probed, respectively, at $E_3=1.8\,\mathrm{eV}$ (solid line) and 1.6 eV (dotted line) in DOO-PPV films.

pump pulse at $t_2=25\,\mathrm{ps}$. As can be seen from the normalized δT decay [Fig. 14(b) inset], the $1B_u$ recovery if any is very slow in comparison to the exciton recombination. Figure 15(a) compares δT dynamics obtained with $E_2=1.6\,\mathrm{eV}$ (solid line) and 1.35 eV (dashed line). In the latter case, an intermediate behavior is observed where both ultrafast and long-lived δT components are present, possibly due to simultaneous excitation of mA_g and kA_g, since PA_1 overlaps with PA_2 (see Fig. 2). We note that varying the probe energy E_3 in the spectral range from 0.6 to 1.1 eV did not affect the observed PM dynamics. We therefore assume in this work that the broad PA_1 band is due to a single mA_g state, which is certainly a naive simplification. The PA_1 band likely consists of a broad continuum of levels resembling the mA_g state found in most calculations on smaller molecules. Because at the moment we cannot identify them as separate levels, we prefer to use the simplest possible picture with a single broad level. Similar considerations apply to the kA_g state.

We find that kA_g relaxation can be probed directly by monitoring transient PA that originates from kA_g at $E_3=1.6-1.8\,\mathrm{eV}$. Fig. 15(b) shows δT decays in DOO-PPV films at $E_3=1.6\,\mathrm{eV}$ (PA_2 range) and $E_3=1.8\,\mathrm{eV}$ (SE range), obtained following reexcitation at $E_2=1.5\,\mathrm{eV}$ ($t_2\approx 16\,\mathrm{ps}$).

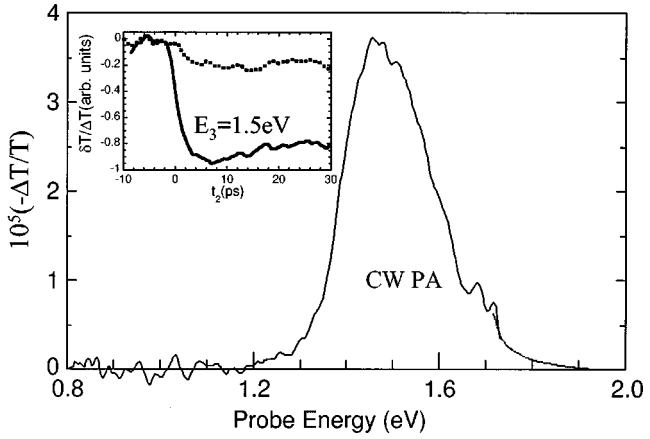

FIG. 16. Steady-state millisecond PM spectrum in DOO-PPV films showing the triplet PA band; the inset shows the PA quenching (δPA) for $E_3=1.5\,\mathrm{eV}$ at $t_3=60\,\mathrm{ps}$ (solid line) and -60 ps (dashed line) caused by the second pump at $E_2=1.6\,\mathrm{eV}$.

In this case δT decay consists of two parts: an ultrafast δPA component lasting 1 ps and a slow δPA (δSE) component for $E_3=1.6\,\mathrm{eV}$ (1.8 eV). We attribute the ultrafast δPA component to the formation and relaxation (within 350 fs) of kA_g. However, kA_g does not relax into $1B_u$, since δSE, δPA_1, and δPA_2 last musch longer (>250 ps). We therefore conclude that kA_g decays with high quantum yield into a relatively long-lived state other than $1B_u$. Similar kA_g relaxation dynamics are observed in polymer solutions.

Few different relaxation routes (other than internal conversion back to $1B_u$) can be envisioned for kA_g.[18] One route is the internal conversion directly to the ground state. The Franck-Condon factors for this nonradiative transition, however, are smaller than those for the $1B_u$ state itself and thus make this process highly improbable. We note that in a smaller molecule like stilbene, internal conversion to the ground state can be facilitated by the cis-trans isomerization (rotation about the CC double bond).[26] In polymers such isomerization is impossible. The second route is singlet fission, where one kA_g singlet exciton decomposes into two triplets with opposite spins.[27] Finally, the third route is exciton dissociation into free charges (or polarons). Both of these last two paths are energetically possible and in fact they may occur concurrently. However, it is known[7] that triplets are characterized by a lifetime of few microseconds at room temperature and a strong PA band peaking at 1.45 eV (Fig. 16). This long-lived PA band is measured in DOO-PPV films at the modulation frequency of 1 kHz, using a steady-state PM setup described elsewhere.[7] Additional production of triplets then should result in increased PA ($\delta T<0$) for $E_3=1.4-1.5\,\mathrm{eV}$; instead, we observe a decrease in PA ($\delta T>0$) in this probe range (Fig. 16 inset). The inset to Fig. 16 shows η vs t_2 for $t_3=60\,\mathrm{ps}$ (solid line) and $t_3=60\,\mathrm{ps}$ (dashed line); PA at $t_3<0$ characterizes the in-phase component long-lived PA at the modulation frequency of 1 MHz. The solid line thus corresponds to the switching efficiency of singlet excitons ($1\,{}^1B_u$), and the dashed line corresponds to the switching efficiency of triplet excitons ($1\,{}^3B_u$). The ratio between the two suggests that only about 75% of reexcited

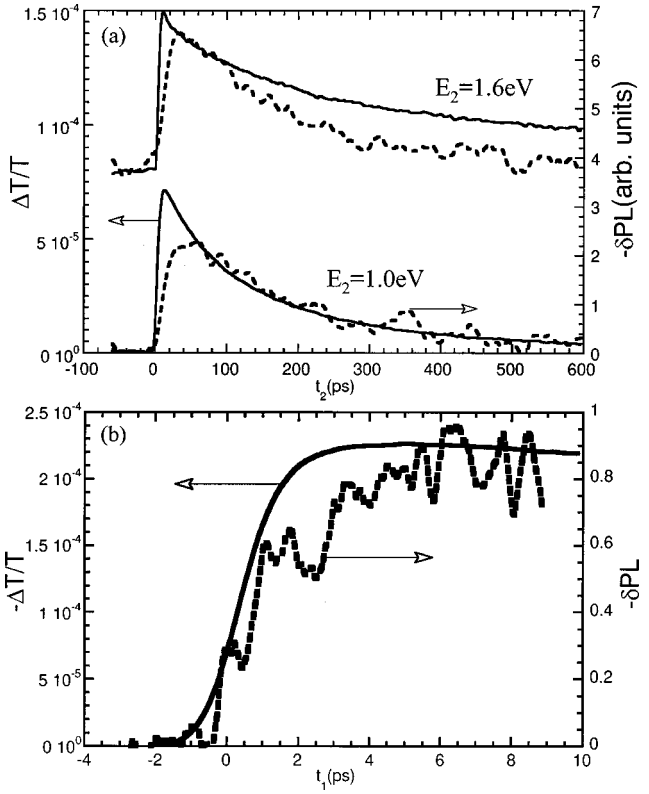

FIG. 17. (a) Correlated δPL (dashed line, right scale) and ΔT (for the second pump) dynamics (solid line, left scale) in DOO-PPV films at $E_2=1.0$ and 1.6 eV; the offset is for clarity. (b) Concurrent δPL (dashed line, right scale) dynamics at $E_2=1.6$ eV and ΔT dynamics (solid line, left scale) measured simultaneously using the probe pulse at $E_3=1.0$ eV in DOO-PPV films.

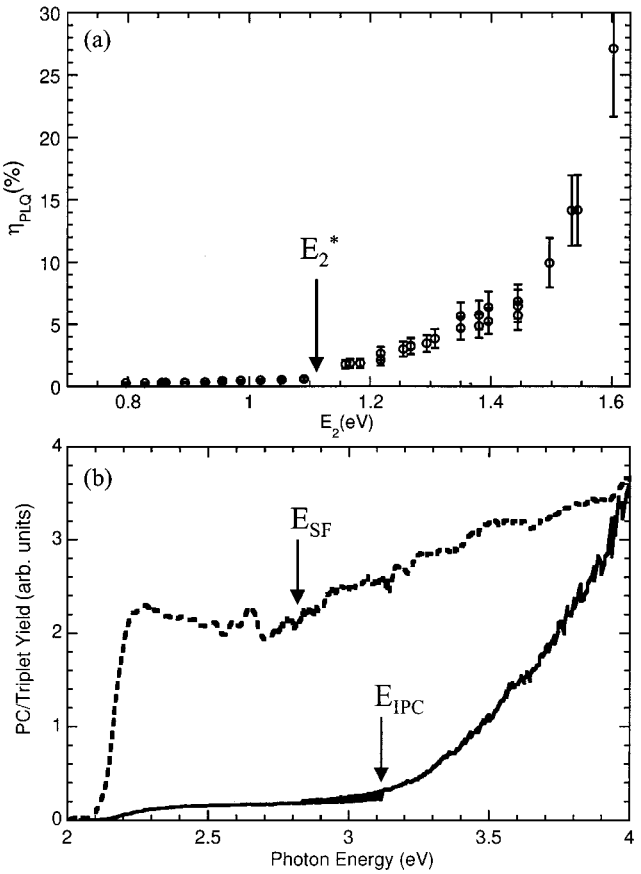

FIG. 18. (a) PL quenching efficiency (η_{PLQ}) spectrum in DOO-PPV films; E_2^* marks the onset of PA_2. (b) Photocurrent (solid line) and triplet PA (dashed line) excitation spectra in DOO-PPV films; E_{SF} marks the singlet fission threshold and E_{IPC} is the onset of the intrinsic PC.

kA_g states ever transform back to $1B_u$. The intermediate state between kA_g and $1B_u$ is likely to have a long lifetime compared to the inverse of the laser pulse repetition rate (12.5 ns), so that its associated PA would not be observed in our transient PM measurements. We can observe a very weak negative δT in DOO-PPV films around $E_3=1.7$ eV at $t_3=100$ ps, where only steady-state population accumulated from several pairs of pump pulses is monitored. These measurements reveal a possible new δPA band extending from 1.6 to 1.8 eV and no correlated contributions at $\sim$0.6 and $\sim$0.15 eV,[28] as expected for free polarons.[29] Thus both scenarios, singlet fission and exciton dissociation, do not appear to be supported by our transient spectroscopy measurements.

In order to elucidate the nature of kA_g relaxation we study changes (δPL) in cw photoluminescence (PL) from the first pump pulse that are induced by the second pump pulse (here PL plays the role of the probe beam). In these measurements we do not use the probe beam. Instead, δPL is measured using the DM technique simultaneously with $\Delta T/T$ (where T is the transmission of the second pump), as shown in Fig. 17(a) for various E_2. While δPL is proportional to the number of quenched excitons, the $\Delta T/T$ magnitude is proportional to the number of reexcited excitons. The decay of δPL versus t_2 follows the $1B_u$ decay; this explains the divergence between δPL and ΔT dynamics at $E_2=1.6$ eV at $t_2>100$ ps. Figure 17(b) compares the δPL decay at $E_2=1.6$ eV and ΔT decay at $E_2=1.0$ eV, measured simultaneously on a short time scale. Even with such a poor signal, it is possible to tell that the δPL onset is delayed with respect to the PA_1 onset. We suggest that the spatial exciton diffusion leads to this effect, i.e., excitons tend to diffuse towards places where exciton quenching (and thus PL quenching) is facilitated.

The ratio between PL switching efficiency (η_{PL}) and PA switching efficiency (η_{PA}) at $t_2=5$ ps is defined as the PL quenching efficiency (η_{PLQ}); both η_{PL} and η_{PA} can be measured simultaneously using the same second pump pulse. For η_{PL} measurements we use the PL signal, whereas for η_{PA} measurements we use an additional probe pulse at $E_3=1.0$ or 2.0 eV. η_{PLQ} is therefore equal to N_A/N_B, where N_A is the number of dissociated kA_g excitons that recombine nonradiatively and N_B is the number of reexcited $1B_u$ excitons. Figure 18(a) shows η_{PLQ} spectrum in DOO-PPV films: PLQ is inefficient at $E_2<1.1$ eV, but it is rather pronounced at $E_2>1.1$ eV. PLQ at $E_2<1.1$ eV may be mediated by defects in this spectral range.[30] However, η_{PLQ} abruptly increases at $E_2^*\approx 1.1$ eV, which corresponds to the edge of the PA_2 band (see Fig. 2). Thus the appearance of a dramatically different recovery dynamics and PL quenching are both associated with the kA_g state.

Next, we correlate the PLQ spectrum with the cw triplet exciton and photoconductivity (PC) excitation spectra in DOO-PPV films, shown in Fig. 18(b). The triplet excitation spectrum is measured at 80 K, using a probe beam tuned at 1.4 eV and a xenon lamp as an excitation source. The PC excitation spectrum is measured using a setup similar to that of Ref. 14. Triplets are mainly produced via intersystem crossing, which is indicated by the steplike triplet yield with an onset at $E(1\ ^1B_u)=2.2$ eV. There is an additional rise in the triplet yield due to singlet fission (SF) ("hot" $1\ ^1B_u \rightarrow 1\ ^3B_u+1\ ^3B_u$) with an onset at $E_{\mathrm{SF}}\equiv 2E[1\ ^3B_u]=2.8$ eV. This rise, however, does not correlate with the PLQ spectrum [Fig. 18(a)]. We note that Ref. 31 suggests that $E[1\ ^3B_u]$ may be significantly larger that the value obtained from the triplet excitation spectrum, in which case the singlet-fission process is even less likely to occur. The PC spectrum, on the other hand, does correlate with the PLQ spectrum: the onset of intrinsic PC (IPC) occurs at $E_{\mathrm{IPC}}=3.2$ eV,[30,32] which is in agreement with the PLQ onset at $E_2^*+E(1\ ^1B_u)\approx 3.3$ eV. These results indicate that PLQ should be associated with exciton dissociation rather than singlet fission. Since similar dynamics are observed in DOO-PPV and PPVD0 dilute solutions, we argue that this dissociation is an intrachain process.

Our data show a clear difference between the mA_g and kA_g relaxation pathways and illustrate the different characters of these states. The classification of A_g states in PPV as consisting of two distinct classes is therefore justified. In the earlier studies[32] mA_g was described as an excited $1B_u$ exciton with energy close to the continuum edge, whereas kA_g was assigned to a biexciton. The latter assignment, however, has been recently questioned.[17] The authors of Ref. 17 use the diagrammatic exciton basis valence-band approach to describe the low-energy excited states in PPV. The low-energy even-parity states are produced as combinations of charge-transfer configurations (one-type excitation, in which an electron is moved to the neighboring unit on the same chain) and triplet-triplet configurations (two-types excitations, which are composed of two coupled triplets on different units with overall zero spin), all of which involve the delocalized MO's (d and d^*) much the same way as B_u states corresponding to bands I and II. The high-energy even-parity states contain configurations of the same charge-transfer one-type-excitations; however, the triplet-triplet configurations here involve both delocalized and localized MO's (d and d^*, l and l^*).

Recent theoretical work[13,14] suggests that special charge-transfer (CT) states may be involved in PC. We speculate that correlation between the PLQ and PC spectra is due to a CT state involved in $k\ ^1A_g$ relaxation. This state in the presence of an electric field dissociates into free carriers (thus producing the observed PC action spectra). Without the field, these carriers remain bound in pairs by Coulomb attraction. The local microscopic field (due to defects, inhomogeneity, photodoping, etc.) may stabilize the formation of bound polaron pairs; this type of excitations has in fact been previously observed in C_{60}-doped[33,34] and pristine PPV films.[35] Some supporting evidence comes from Fig. 17(b), which shows the delayed onset of δPL with respect to $\Delta \mathrm{PA}_1$. This delay may be due to the time necessary to reach an appropriate position on the chain, e.g., close to a kink, which would then not only facilitate exciton dissociation, but also prevent the subsequent radiative recombination.

Although it has been shown[17] that both $m\ ^1A_g$ and $k\ ^1A_g$ have a charge-transfer character, it appears that only $k\ ^1A_g$ assists exciton dissociation. The $k\ ^1A_g$ state, unlike $m\ ^1A_g$, contains contributions from l and l^* (these come from the triplet-triplet configurations).[17] The same MO's appear in band III in Fig. 1; they are believed to assist electron-hole separation.[13,14] We argue that $k\ ^1A_g$ may possess similar properties and also assist charge separation. Alternatively, $k\ ^1A_g$ may relax into another intermediate CT state, facilitating polaron pair formation. Earlier theoretical work indicated the existence of a dipole-forbidden state near band II (Fig. 1), produced by an antisymmetric combination of delocalized and localized MO's involved in the formation of band III, i.e., $d \rightarrow l^* - 1 \rightarrow d^*$.[9,10] This state cannot be accessed directly from the ground state via B_u-type excitations; however, it may couple to $k\ ^1A_g$, providing an efficient route for exciton dissociation. Our results suggest that the PC action spectrum measured by two-photon absorption spectroscopy may provide further insights into the correlation found here between the kA_g states and PC excitation spectrum.

VI. CONCLUSIONS

In summary, we have studied ultrafast relaxation processes of B_u and A_g exciton states, which are known to play a dominant role in the photophysics of π-conjugated polymers. The B_u states can be studied using a regular pump-and-probe spectroscopy, whereas the A_g states require new spectroscopic methods. We have used a three-beam transient photomodulation technique to uniquely probe the relaxation dynamics of two-photon allowed states. Two different classes of A_g states are distinguished: one class (mA_g) experiences ultrafast internal conversion back to the lowest singlet exciton, whereas the other class (kA_g) in violation of the Vavilov-Kasha rule undergoes a different relaxation pathway. Ensuing exciton dissociation into a long-lived polaron pair results in PL quenching with the action spectrum similar to that of intrinsic photoconductivity. It is a demonstration of direct all-optical exciton dissociation without the assistance of defects or electric field. We argue that the kA_g state may belong to the charge-transfer states that mediate carrier photogeneration.

ACKNOWLEDGMENTS

We thank R. Meyer for the two-photon absorption spectrum of DOO-PPV and M. C. DeLong and G. Levina for the linear absorption spectrum of DOO-PPV. The work at Utah was supported in part by the DOE, Contract No. DE-FG03-93ER 45490.

[1] S. N. Dixit, D. Guo, and S. Mazumdar, Phys. Rev. B **43**, 6781 (1991); Z. G. Soos, S. Etemad, D. S. Galvao, and S. Ramasesha, Chem. Phys. Lett. **194**, 341 (1992).
[2] R. Kersting, U. Lemmer, R. F. Mahrt, K. Leo, H. Kurz, H. Bassler, and E. O. Gobel, Phys. Rev. Lett. **70**, 3820 (1993); **73**, 1440 (1994).
[3] J. B. Birks, *Photophysics of Aromatic Molecules*, (Wiley-Interscience, London, 1970).
[4] N. T. Harison, G. R. Hayes, R. T. Phillips, and R. H. Friend, Phys. Rev. Lett. **77**, 1881 (1996).
[5] S. V. Frolov, Ch. Kloc, S. Berg, G. Thomas, and B. Batlogg, Chem. Phys. Lett. **326**, 558 (2000).
[6] M. Pope and C. E. Swenberg, *Electronic Processes in Organic Crystals and Polymers* (Oxford University Press, New York, 1999).
[7] S. V. Frolov, M. Liess, P. A. Lane, W. Gellermann, Z. V. Vardeny, M. Ozaki, and K. Yoshino, Phys. Rev. Lett. **78**, 4285 (1997).
[8] Z. Bao, K. R. Amundson, and A. J. Lovinger, Macromolecules **31**, 8647 (1998).
[9] M. Chandross, S. Mazumdar, M. Liess, P. A. Lane, Z. V. Vardeny, M. Hamaguchi, and K. Yoshino, Phys. Rev. B **55**, 1486 (1997).
[10] M. J. Rice and Yu. N. Garstein, Phys. Rev. Lett. **73**, 2504 (1994).
[11] J. Cornil, D. Beljonne, R. H. Friend, and J. L. Bredas, Chem. Phys. Lett. **223**, 82 (1994).
[12] M. Liess, S. Jeglinski, Z. V. Vardeny, M. Ozaki, K. Yoshino, Y. Ding, and T. Barton, Phys. Rev. B **56**, 15 712 (1997).
[13] S. Mukamel, S. Tretiak, T. Wagersreiter, and V. Chernyak, Science **277**, 781 (1997).
[14] A. Köhler, D. A. D. A. dos Santos, D. Beljonne, Z. Shuai, J.-L. Bredas, A. B. Holmes, A. Kraus, K. Mullen, and R. H. Friend, Nature (London) **392**, 903 (1998).
[15] R. Meyer, Ph.D. thesis, University of Utah, 1996.
[16] W. Barford, R. J. Bursill, and M. Yu. Lavrentiev, J. Phys.: Condens. Matter **10**, 6429 (1998); M. Yu. Lavrentiev, W. Barford, S. J. Martin, H. Daly, and R. J. Bursill, Phys. Rev. B **59**, 9987 (1999).
[17] A. Chakrabarti and S. Mazumdar, Phys. Rev. B **59**, 4839 (1999).
[18] S. V. Frolov, Z. Bao, M. Wohlgenannt, and Z. V. Vardeny, Phys. Rev. Lett. **85**, 2196 (2000).
[19] L. J. Rothberg, M. Yan, F. Papadimitrakopoulos, M. E. Galvin, E. W. Kwock, and T. M. Miller, Synth. Met. **80**, 41 (1996).
[20] S. V. Frolov, W. Gellermann, Z. V. Vardeny, M. Ozaki, and K. Yoshino, Synth. Met. **84**, 493 (1997).
[21] U. Mizrahi, I. Shtrichman, D. Gershoni, E. Ehrenfreund, and Z. V. Vardeny, Synth. Met. **102**, 1182 (1999).
[22] S. Heun, R. F. Mahrt, A. Greiner, U. Lemmer, H. Bassler, D. A. Halliday, D. D. C. Bradley, P. L. Burns, and A. B. Holmes, J. Phys.: Condens. Matter **5**, 247 (1993).
[23] T.-Q. Nguyen, J. Wu, V. Doan, B. J. Schwartz, and S. H. Tolbert, Science **288**, 652 (2000).
[24] R. A. J. Janssen, in *Primary Photoexcitations in Conjugated Polymers: Molecular Exciton versus Semiconductor band model* (World Scientific, Singapore, 1997).
[25] S. V. Frolov and Z. V. Vardeny, Rev. Sci. Instrum. **69**, 1257 (1998).
[26] M. Klessinger and J. Michl, *Excited States and Photochemistry of Organic Molecules* (VCH, New York, 1995).
[27] M. Wohlgenannt, W. Graupner, R. Osterbacka, G. Leising, D. Comoretto, and Z. V. Vardeny, Synth. Met. **101**, 267 (1999).
[28] P. A. Lane, X. Wei, and Z. V. Vardeny, Phys. Rev. Lett. **77**, 1544 (1996).
[29] W. Graupner, G. Cerullo, G. Lanzani, M. Nisoli, E. J. W. List, G. Leising, and S. De Silvestri, Phys. Rev. Lett. **81**, 3259 (1998).
[30] S. Barth and H. Bässler, Phys. Rev. Lett. **79**, 4445 (1997).
[31] Yu. V. Romanovskii, A. Gerhard, B. Schweitzer, U. Scherf, R. I. Personov, and H. Bässler, Phys. Rev. Lett. **84**, 1027 (2000).
[32] J. M. Leng, S. Jeglinski, X. Wei, R. E. Benner, Z. V. Vardeny, F. Guo, and S. Mazumdar, Phys. Rev. Lett. **72**, 156 (1994).
[33] B. Kraabel, C. H. Lee, D. McBranch, D. Moses, N. S. Sariciftci, and A. J. Heeger, Chem. Phys. Lett. **213**, 389 (1993).
[34] S. V. Frolov, P. A. Lane, M. Ozaki, K. Yoshino, and Z. V. Vardeny, Chem. Phys. Lett. **286**, 21 (1998).
[35] M. Yan, L. J. Rothberg, F. Papadimitrakopoulos, M. E. Galvin, and T. M. Miller, Phys. Rev. Lett. **72**, 1104 (1994); M. Yan, L. J. Rothberg, E. W. Kwock, and T. M. Miller, *ibid.* **75**, 1992 (1995).